Reduction of efficiency droop in InGaN-Based UV Light-Emitting Diodes with InAlGaN Barrier

Ching-Hsueh Chiu[1], Po-Min Tu[1], Jet-Rung Chang[2], Wei-Ting Chang[3], Hao-Chung Kuo[1,*], Chun-Yen Chang[2]

[1]Department of Photonics and Institute of Electro-Optical Engineering, National Chiao-Tung University, Hsinchu 300, Taiwan

[2]Institute of Electronics, National Chiao-Tung University, Hsinchu 300, Taiwan.

[3]Department of Electro-Physics, National Chiao-Tung University, Hsinchu 300, Taiwan
TEL: +886-3-5712121#56354,
Tai-wan* hckuo@faculty.nctu.edu.tw

ABSTRACT

In this study, we fabricated and compared the performance of LEDs of InGaN-based UV MQWs active region with ternary AlGaN and quaternary InAlGaN barrier layers. HRXRD and TEM measurements show the two barriers are consistent with the lattice, and smooth morphology of quaternary InAlGaN layer can be observed in AFM. The electroluminescence results indicate that the light performance of the InGaN-based UV LEDs can be enhanced effectively when the conventional LT AlGaN barrier layers are replaced by the InAlGaN barrier layers. Furthermore, simulation results show that InGaN-based UV LEDs with quaternary InAlGaN barrier exhibit higher radiative recombination rate about 62% and low efficiency droop about 13% at a high injection current. We attribute this change to a drastic improvement from increasing of carrier concentration and redistribution of carriers, because of reduction of scatterings due to better morphology in the transverse carrier transport through the InGaN/InAlGaN MQWs.

Keywords: UV LEDs, efficiency droop

INTRODUCTION

GaN-based ultraviolet light emitting devices (LEDs) have attracted great attention in last few years due to its potential applications in photocatalytic deodorizing such as air conditioner,[1] and there have been interests in solid-state lighting by using near-UV LEDs light for the phosphorconverting source.[2,3] However, external quantum efficiency (EQE) decreases drastically below the wavelength of 400 nm.[4] It is well known that in low indium content InGaN quantum wells (QWs), AlGaN barrier is necessary for carrier confinement. But the two materials of AlGaN and InGaN are very different in growth temperature, which affects strongly on the quality of material and device performances. To improve the quantum efficiency of the InGaN-based LEDs, previous reports used InAlGaN in the quantum barrier instead of AlGaN or GaN for polarization, strain, material quality, and interfacial abruptness issues.[5–8] However, by introducing of indium in AlGaN without increase aluminum content will cause the enhancement of the quantum confined Stark effect and other band gap issues. In this letter, the InAlGaN barrier was not for lattice or band gap matched in InGaN QW but matched in optimized AlGaN barrier, for a fair investigation on the light output and efficiency current droop characteristics.

EXPERIMENTS

All samples used in this letter were grown on 2 inch c-plane sapphire substrates using an atmospheric-pressure metal organic chemical vapor deposition (SR4000) system. For the growth of GaN-based LEDs, trimethyl gallium (TMGa), trimethyl indium (TMIn), trimethyl aluminum (TMAl), and ammonia (NH3) were used as the source precursors for Ga, In, Al, and N, respectively. Silane (SiH4) and biscyclopentadienyl magnesium (Cp2Mg) were used as n-type and p-type dopants. The conventional structure is as follows. A 500 °C LT 30-nm-thick GaN nucleation layer was deposited, followed by a 1-μm-thick undoped GaN layer and a 2.5-μm-thick n-type $Al_{0.02}Ga_{0.98}N$ layer grown at 1150 °C. A ten-period InGaN/AlGaN multi-QW (MQW) active region was grown at 830 °C. Subsequently, a 15-nm-thick Mgdoped $Al_{0.3}Ga_{0.7}N$ and a 10-nm-thick Mg-doped $Al_{0.1}Ga_{0.9}N$ electron-blocking layers (EBLs) were grown at 1050 °C, followed by a 60-nm-thick Mg-doped GaN contact layer grown at 1030 °C. The quaternary structure of InGaN/InAlGaN MQW was almost identical to that of the InGaN/AlGaN MQW LED, the only difference was that we used InAlGaN instead of AlGaN as the barrier layers in the active region. Here, the MQW active region consisted of ten periods of 2.6-nm-thick undoped $In_{0.025}Ga_{0.975}N$ well layers and 11.7-nm-thick Si-doped $In_{0.0085}Al_{0.1112}Ga_{0.8803}N$ or $Al_{0.08}Ga_{0.92}N$ barrier layers growth on n-$Al_{0.02}Ga_{0.98}N$/ud-GaN/sapphire. During the growth of barriers, we kept the flow rates of TMGa, NH3, and SiH4 at 12.24 μmol/min, 0.67 mol/min, and 0.196 nmol/min. For the growth of InAlGaN, we added the flow rate of TMIn for 0.79 μmol/min and increased the flow rate of TMAl from 1.94 μmol/min to 2.13 μmol/min, compared to AlGaN barrier. To probe the detailed properties of epitaxial layers, a 50 nm InAlGaN and AlGaN single heteroepitaxial layers were also deposited on n-AlGaN/ud-GaN/sapphire substrate. The mole fractions of Al and In in MQWs were identified by double crystal x-ray diffraction (DCXRD, Bede D1, U.K.) using Cu Kα1 (λ=1.54056 Å) as source. These samples were also characterized by photoluminescence (PL), atomic force microscopy (AFM) and transmission electron microscopy (TEM) to reveal the optical property, surface morphology, and MQWs structure, respectively. Finally, the UV LED wafers were processed into mesa-type chips (size: 1 mm x1 mm) and packaged on epoxy-free metal cans (TO-66, thermal resistance (R_θ)~2 K/W). The output power of the UV LED was measured using an integrated sphere detector and tested at room temperature with currents up to 1 A. Testing is done in pulsed mode with 100 μs pulses and a 1% duty cycle to prevent self-heating because the thermal time constant of the LEDs is in the millisecond range.[9] In this letter, the optical and electrical properties of InGaN/InAlGaN and conventional InGaN/AlGaN MQW LEDs are numerically calculated using the APSYS simulation software.[10]

RESULTS AND DISCUSSION

PL spectra of AlGaN and InAlGaN single heteroepitaxial layers grown on n-AlGaN/ud-GaN/sapphire substrate were obtained at a room temperature to investigate the band edge emission. Figure 1 shows that the PL emission energy of these two samples are very close (about 3.594 eV) and the peak intensity of InAlGaN is slightly higher than AlGaN. The strong PL emission is attributed to the better crystal quality. Inset in Fig. 1 shows the surface morphology of the two AlGaN and InAlGaN single heteroepitaxial layers with the same thickness about 50 nm. The root-mean-square (RMS) roughness measured by AFM is about 0.813 nm and 0.595 nm, respectively. The relatively high roughness of Al-GaN

single heteroepitaxial layer can mainly be attributed to the low deposition temperature of 830 °C necessary for the adjacent InGaN well. Figure 2(a) shows the XRD (ω-2θ) curves in the (002) reflections of InGaN/AlGaN and InGaN/InAlGaN MQWs. The results show that the locations of multiple satellite peaks of InGaN/AlGaN and InGaN/InAlGaN MQWs are very close. This indicates that the thickness of barrier layer in these two samples is matched and it is quite consistent with the measured values of 11.7 nm from HRTEM images as shown in Figs. 2(b) and 2(c). In addition to experimentally estimate the indium and aluminum composition in the MQWs, we simulate the XRD (ω-2θ) curve by using dynamical diffraction theory. The In composition in the QWs was determined to be about 2.5%, where the thickness of the well was about 2.6 nm. The compositions of ternary and quaternary barriers were $Al_{0.08}Ga_{0.92}N$ and $In_{0.0085}Al_{0.1112}Ga_{0.8803}N$, respectively. Besides, the growth rates of well and barrier were estimated about 0.329 Å/s and 0.308 Å/s, respectively.
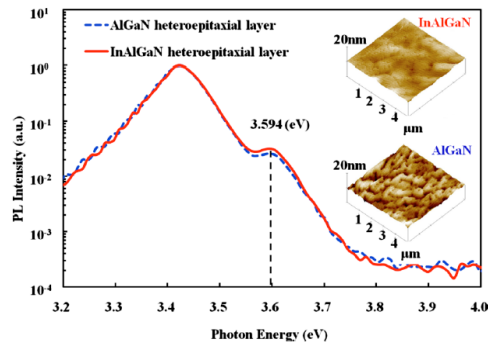

FIG. 1. (Color online) Room-temperature PL spectra of AlGaN and InAlGaN single heteroepitaxial layers. Inset in Fig. 1 shows surface morphology AFM over 5×5 μm² of AlGaN (RMS: 0.813 nm) and InAlGaN (RMS: 0.595 nm) layer with thickness about 50 nm.

The optical properties of UV LED with ternary and quaternary barrier are shown in Fig. 3. Figure 3(a) shows the light output power-current-voltage (L-I-V) characteristics for the AlGaN and InAlGaN barrier UV LEDs. The forward voltage was 3.89 V and 3.98 V for InGaN/AlGaN and InGaN/InAlGaN MQWs UV LED at a forward current of 350 mA, respectively. A little high forward voltage of InAlGaN barrier LED can be attributed to the higher Al content compare to the AlGaN barrier, thus increase the series resistance in the device. The light output power of InGaN-based UV LED with the InAlGaN barrier is higher by 25% and 55% than the AlGaN barrier at 350 mA and 1000 mA, respectively. Figure 3(b) shows the normalized efficiency curves of experimental (open circles) and simulated (solid lines) as a function of forward current for the two samples. For the InGaN/AlGaN UV LEDs, when the injection current exceeds 1000 mA, the efficiency is reduced to 66% of its maximum value. In contrast, InGaN/InAlGaN UV LEDs exhibit only 13% efficiency droop when we increase the injection current to 1000 mA. The reduction in efficiency droop is quite clear and the current at maximum efficiency shifts from 150 to 400 mA. Besides, the wavelength is nearly constant about 380 nm over the entire current range. The absence of temperature-induced redshift suggests that selfheating is substantially suppressed by using metal type packaging and pulsed mode operating.[11] In order to investigate the physical origin of efficiency droop in these UV LEDs, we performed a simulation of the above structures by using the APSYS simulation software. Commonly accepted Shockley–Read–Hall recombination lifetime (about ~6 ns) and Auger recombination coefficient (about ~10^{-30} cm^6 s^{-1}) are used in the simulations. Other material parameters of the semiconductors used in the simulation can be found in Ref. 12. In addition, we can reduce the effect of spontaneous and

piezoelectric polarizations because of lattice match condition in barrier between AlGaN and InAlGaN. The total polarization fields in different combination of materials can be obtained through the calculation, and the results of $In_{0.025}Ga_{0.975}N$, $Al_{0.08}Ga_{0.92}N$, and $In_{0.0085}Al_{0.1112}Ga_{0.8803}N$ are the -0.0305 (C m^{-2}), -0.0391 (C m^{-2}), and -0.0398 (C m^{-2}), respectively.[13] Besides, a different bandoffset ratio from 6:4 to 7:3 is used in this simulation for introducing of indium in AlGaN. We can know that under the same energy band of barrier, the band-offset ratio from 6:4 to 7:3 will lead higher conduction-band and lower valence-band between well and barrier. This is useful for electron confinement and hole distribution in low indium content InGaN-based UV LEDs. However, another difficult problem is the inclusion of degenerate valence bands in minority carrier hole mobility. Hence, to investigate the efficiency droop in these two samples, we assume that InGaNbased UV LED with InAlGaN barrier has relatively high carrier mobility. The values of mobility for electron and hole are assumed in the simulation, $\mu_{n\text{-}InGaN/AlGaN}=354$ cm^2 /V s, $\mu_{n\text{-}InGaN/InAlGaN}=642$ cm^2 /V s, $\mu_{p\text{-}InGaN/AlGaN}=2$ cm^2 /V s, and $\mu_{p\text{-}InGaN/InAlGaN}=5$ cm^2 /V s, respectively. Finally, the results of the EQE droop simulation of both different structures are in good agreement with the experimental data as shown in Fig. 3(b). Finally, we have to check the actual carrier distribution in our simulation.
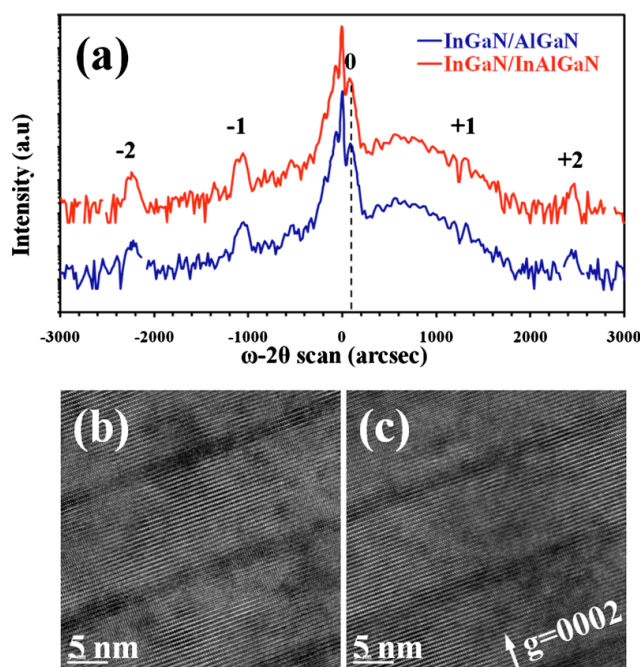

FIG. 2. (Color online) (a) XRD ω-2θ curves in the (002) reflections of InGaN/AlGaN and InGaN/InAlGaN MQW. Cross-sectional TEM images of (b) InGaN/AlGaN and (c) InGaN/InAlGaN MQW. The diffraction condition is g=0002.
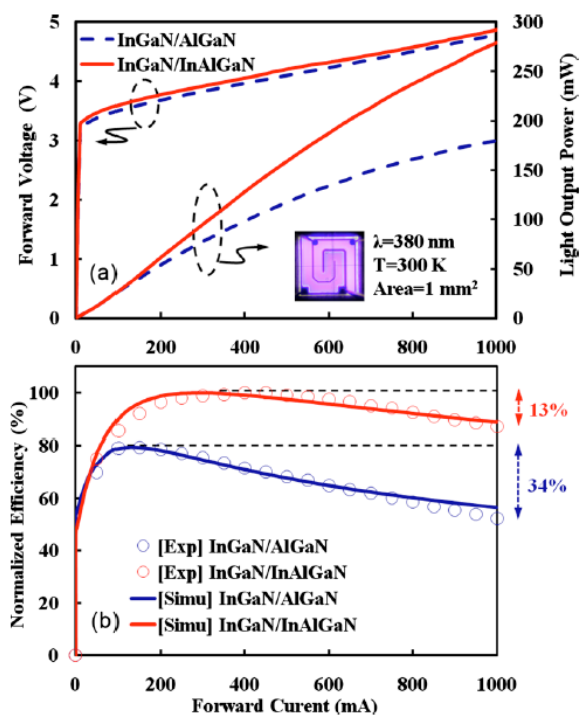
FIG. 3. (Color online) (a) L-I-V curves of the LEDs with AlGaN (dash) and InAlGaN (solid) barrier. (b) Normalized efficiency curves of experimental (open circles) and simulated (solid lines). Inset in Fig. 3(a) shows the mesatype UV chip.

Figure 4 shows the calculated carrier distribution in these UV LEDs structure under a high forward current density of 100 A/cm^2 (1000 mA) by APSYS. When we apply the corresponding band-offset ratio and the carrier mobility in InGaN/InAlGaN MQWs, the electron and hole concentration increases in the QW by about 26% and 35%, respectively,

and the distribution of carrier becomes more uniform than InGaN/AlGaN case. Under high current density, the carrier distribution of both electrons and holes determines how efficient the photon-emission process will be. As shown in Fig. 4, the peak-to-peak carrier ratio of InAlGaN barrier sample is reduced due to better carrier transportation and this is also more obvious in the hole distribution. The direct consequence is the increasing radiative recombination rate and thus the light output is expected to rise. On the other hand, in the traditional AlGaN barrier samples, the holes are locally concentrated in the first QW, which causes the unbalanced distribution between different types of carriers and thus leads to reduction in radiative recombination rate. Comparing electrons and holes, holes suffer more as a result of this nonuniformity due to their large effective mass and low mobility. Thus, our InAlGaN design can reduce the carrier leakage and increase electron-hole pair radiative recombination simultaneously, especially for the distribution of holes.
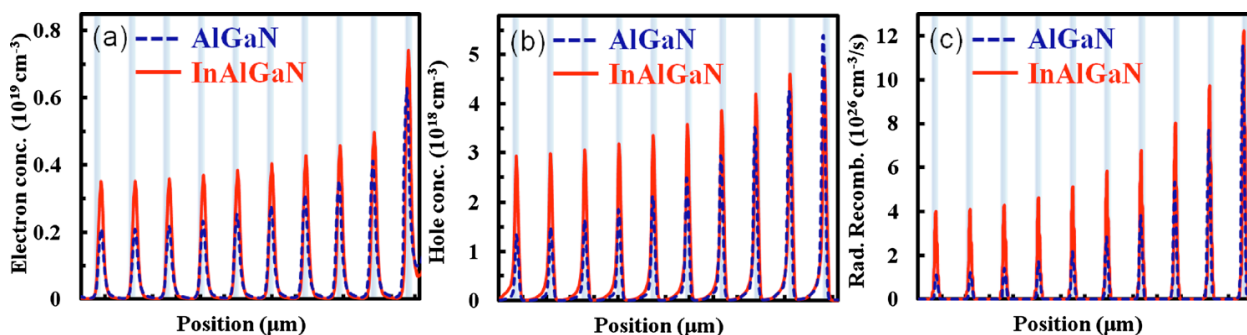

FIG. 4. (Color online) Distribution of (a) electron, (b) hole concentrations, and © radiative recombination rates concentrations of the LEDs with AlGaN and InAlGaN barrier under a high forward current density of 100 A/cm2.

SUMMARY

The efficiency droop in InGaN-based UV LED with AlGaN and InAlGaN barrier is investigated. Electroluminescence results indicate that the light performance of quaternary LEDs can be enhanced about 25% and 55% under 350 mA and 1000mA, respectively. Furthermore, simulations show that quaternary LEDs exhibit higher radiative recombination rate about 62% and low efficiency droop about 13% at a high injection current. We attribute this change to a drastic improvement from increasing of carrier concentration and redistribution of carriers, because of reduction of scatterings due to better morphology in the transverse carrier transport through the InGaN/InAlGaN MQWs.

ACKNOWLEDGMENT

REFERENCES

[1] A. Sandhu, Nat. Photonics 1, 38 (2007).

[2] Y. S. Tang, S. F. Hu, C. C. Lin, N. C. Bagkar, and R. S. Liu, Appl. Phys. Lett. 90, 151108 (2007).

[3] Y. C. Chiu, W. R. Liu, C. K. Chang, C. C. Liao, Y. T. Yeh, S. M. Jang, and T. M. Chen, J. Mater. Chem. 20, 1755

(2010).

[4]H. Hirayama, J. Appl. Phys. **97**, 091101 (2005).

[5]A. Knauer, H. Wenzel, T. Kolbe, S. Einfeldt, M. Weyers, M. Kneissl, and G. Tränkle, Appl. Phys. Lett. **92**, 191912 (2008).

[6]M. F. Schubert, J. Xu, J. K. Kim, E. F. Schubert, M. H. Kim, S. Yoon, S. M. Lee, C. Sone, T. Sakong, and Y. Park, Appl. Phys. Lett. **93**, 041102 (2008).

[7]J. J. Wu, G. Y. Zhang, X. L. Liu, Q. S. Zhu, Z. G. Wang, Q. J. Jia, and L. P. Guo, Nanotechnology **18**, 015402 (2007).

[8]S. H. Baek, J. O. Kim, M. K. Kwon, I. K. Park, S. I. Na, J. Y. Kim, B. J. Kim, and S. J. Park, IEEE Photon. Technol. Lett. **18**, 1276 _2006_.

[9]Q. Shan, Q. Dai, S. Chhajed, J. Cho, and E. F. Schubert, J. Appl. Phys. **108**, 084504 (2010).

[10]APSYS by Crosslight Software Inc., Burnaby, Canada: http://www.crosslight.com.

[11]Y. Yang, X. A. Cao, and C. Yan, IEEE Trans. Electron Devices **55**, 1771 (2008).

[12]F. Bernardini, in *Nitride Semiconductor Devices: Principles and Simulation*, edited by J. Piprek _Wiley, New York, 2007_, pp. 49–67.

[13]M. H. Kim, M. F. Schubert, Q. Dai, J. K. Kim, E. F. Schubert, J. Piprek, and Y. Park, Appl. Phys. Lett. **91**, 183507 (2007).